1575 K using the unit cell volume of Zn_2SiO_4 at 298 K (1577.8 Å^3) and substituting iron for zinc in the formula unit (the number of formula units of Zn_2SiO_4 in the unit cell of the willemite structure is 18). The small difference between the value derived by this method (3.86 g cm^{-3}) and the experimentally determined value (3.75 g cm^{-3}) can be accounted for by increasing Fe–O–Si angles or allowing for the slightly longer Fe–O bond (≈1.98 Å) relative to the Zn–O bond (≈1.958 Å) (*25*) in the model.
29. W. E. Jackson *et al.*, *Eos* **71**, 1665 (1990); in preparation.
30. T. N. Irvine and I. Kushiro, *Carnegie Inst. Washington Yearb.* **75**, 668 (1976); A. J. Irving, *Geochim. Cosmochim. Acta* **42**, 743 (1978).
31. R. G. Burns and W. S. Fyfe, in *Researches in Geochemistry*, vol. 2, P. H. Abelson, Ed. (Wiley, New York, 1967), pp. 259–285.
32. R. G. Burns, *Mineralogical Applications of Crystal Field Theory* (Cambridge Univ. Press, Cambridge, 1970), pp. 109–112.
33. L. Galoisy and G. Calas, *Am. Mineral.* **76**, 1777 (1991); *Geochim. Cosmochim. Acta*, in press.
34. F. Farges, G. E. Brown Jr., G. Calas, L. Galoisy, G. A. Waychunas, in preparation.
35. H. S. Waff, *Geophys. Res. Lett.* **2**, 193 (1975).
36. D. L. Farber and Q. Williams, *Science* **256**, 1427 (1992).
37. We thank S. Bohlen for providing the synthetic fayalite for this study, S. Cramer for assisting in the data collection, and M. Brandriss and E. Winterburn for assisting in the sample characterization. Helpful reviews were provided by J. I. Brauman and J. F. Stebbins and by two anonymous referees. This work was supported by the National Science Foundation (Stanford) and the Department of Energy (Los Alamos).

26 July 1993; accepted 6 August 1993

Teosinte glume architecture 1: A Genetic Locus Controlling a Key Step in Maize Evolution

Jane Dorweiler, Adrian Stec, Jerry Kermicle, John Doebley*

Teosinte, the probable progenitor of maize, has kernels that are encased in hardened fruitcases, which interfere with the use of the kernels as food. Although the components of the fruitcase are present in maize, their development is disrupted so that the kernels are not encased as in teosinte but exposed on the ear. The change from encased to exposed kernels represents a key step in maize evolution. The locus that largely controls this morphological difference between maize and teosinte, *teosinte glume architecture 1*, is described and genetically mapped.

Genetic and biosystematic research has provided substantial evidence that maize is a domesticated derivative of the wild Mexican grass teosinte (*Zea mays* ssp. *parviglumis*) (*1*–*6*). Nevertheless, because of the profound architectural differences between the maize and teosinte ears, the precise morphogenetic steps involved in the transition from teosinte to maize remain in doubt (*7*–*9*). In this report we describe a genetic locus, *teosinte glume architecture 1* (*tga1*), that controls a key difference in ear development between teosinte and maize: It alters the development of the teosinte cupulate fruitcase so that the kernel is exposed on the ear for easy harvest. The existence of this locus supports the view (*1*, *7*) that a small number of single-gene changes could account for the transformation of teosinte into maize.

The cupulate fruitcase of teosinte is composed of a rachis internode (or rachid) and the attached spikelet (Fig. 1). In the teosinte ear, the rachids are deeply invaginated such that the mature spikelet (including the kernel) fits within this invagination, or cupule. The spikelet is composed of a female flower and a series of bracts that subtend it. The lowest of these bracts is the outer glume, which seals the opening to the cupule so that the kernel is obscured from view and protected from pests and granivores. At maturity, the rachid and the outer glume become extremely hardened (indurated), giving the cupulate fruitcase the appearance of a polished pebble. In maize, the rachid and glume are present but do not form a casing around the kernel, which is instead exposed on the ear for easy harvest.

J. Dorweiler, A. Stec, J. Doebley, Department of Plant Biology, University of Minnesota, St. Paul, MN 55108. J. Kermicle, Laboratory of Genetics, University of Wisconsin, Madison, WI 53706.

*To whom correspondence should be addressed.

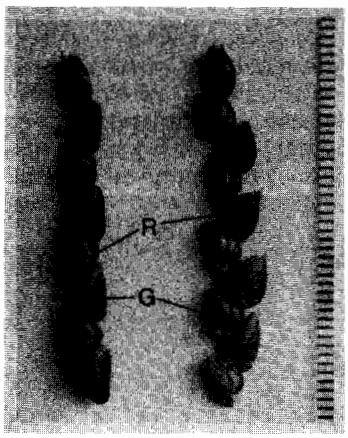

Fig. 1. Ear of pure teosinte composed of eight cupulate fruitcases (left) and an ear of teosinte homozygous for the maize allele at *tga1* (right). The rachids (R) of teosinte are fully developed, forming a deep invagination in which the kernels are housed. The glume (G) seals the opening of the invagination so that the kernel is completely hidden and protected. The rachids of teosinte with the maize allele at *tga1* are less developed, forming only a short, shallow invagination that does not fully encase the kernel. The scale bar to the right is in millimeters.

We (*10*) identified a quantitative trait locus (QTL) on chromosome 4 controlling 42 to 50% of the phenotypic variance for outer glume induration and hypothesized that this locus represented a single gene with a dramatic phenotypic effect. This QTL appears to correspond to a factor affecting glume induration on chromosome 4 previously identified by other investigators (*11*). To investigate this QTL further, we transferred the segment of maize (Race Reventador, NAY-15) chromosome 4 containing this QTL into teosinte (Z. *mays* ssp. *parviglumis* Iltis and Cochrane 1981) by three generations of backcrossing coupled with positive selection for molecular-marker loci [restriction fragment length polymorphisms (RFLPs)] in the region flanking the QTL (Fig. 2). We also exercised negative selection on the maize alleles at RFLP loci outside the target region, enabling us to recover the teosinte (recurrent parent) genome rapidly. Similarly, we transferred the segment of teosinte (Z. *mays* ssp. *mexicana* Wilkes 48703) chromosome 4 containing this QTL into maize inbred line W22 by six generations of backcrossing. After the sixth backcross generation, a true-breeding line (W22-TGA) was recovered that possessed the W22 plant morphology except for the teosinte-like glumes in its ears.

To investigate this QTL, a segregating F_2 population was derived from the crossing of W22-TGA with the recurrent parent (W22). Of 230 F_2 progeny, 212 were scored for both glume induration and nine RFLP loci. The remaining 18 were scored only for

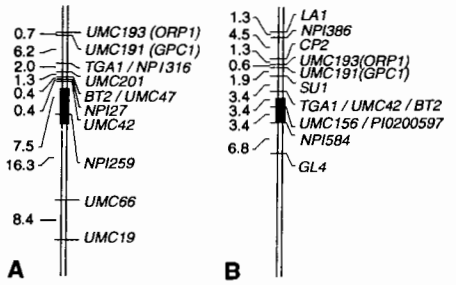

Fig. 2. Linkage maps of a portion of chromosome 4 showing the position of *tga1* and the marker loci used to localize it. Results from (**A**) the W22 × W22-TGA F_2 population and (**B**) the *la1-su1-gl4* (Maize Genetics Stock Center) × W22-TGA population. Black rectangles indicate the region in which the centromere is located.

RFLPs because they were barren (lacked ears) or because their ears were lost to pests. Glume induration segregated in two discrete classes as expected for a trait controlled by a single Mendelian locus (*12*). This result demonstrated that the QTL represents a single locus, thereby confirming our inference (*10*) that a single locus of large effect controls much of the difference in glume induration between maize and teosinte. The use of RFLP loci allowed us to map *tga1* close to the centromere on the short arm of chromosome 4 (Fig. 2A).

We also mapped *tga1* relative to the classical genetic loci, *lazy plant 1* (*la1*), *sugary 1* (*su1*), and *glossy 4* (*gl4*). We crossed W22-TGA to an *la1-su1-gl4* stock, then backcrossed the hybrid to the *la1-su1-gl4* stock. Of the 156 backcross progeny examined, 19 showed recombination between the marker loci. These 19 plants were subsequently test-crossed to W22-TGA, and the progeny of these crosses were classified as having indurate or nonindurate glumes (Fig. 2B). The combined results of both mapping populations place *tga1* on the short arm of maize chromosome 4 between *su1* and *brittle endosperm 2* (*bt2*). In both populations, the maize allele (*Tga1*) behaved in a dominant fashion to the teosinte allele (*tga1*).

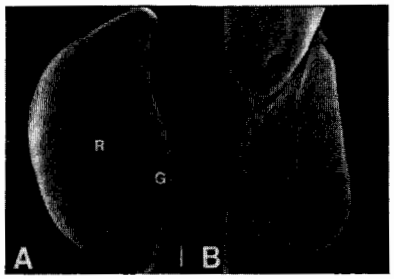

Fig. 3. Scanning electron micrographs of single fruitcases of (**A**) teosinte and (**B**) teosinte homozygous for the maize allele at *tga1*, both collected just before pollination. The maize allele makes the rachid more short and narrow, exposing more of the outer glume. In teosinte, the glume arches into the cupule, whereas the maize allele causes the glume to be oriented directly upward at this stage. The scale bar represents 0.5 mm.

The maize allele in a teosinte background reveals the effects of this locus on the normal teosinte ear and provides a view of what may have been one of the steps in the early evolution of maize. In this background, *Tga1* makes the cupules shorter, less deeply invaginated (Fig. 3), and unable to accommodate the mature spikelet and kernel that become partially exposed (Fig. 1). The outer glume is altered so that it is oriented upward (parallel to the axis of the ear) rather than partially inward (literally into the cupule) (Fig. 3). As a result, the kernel is not held tightly within the cupule at maturity but is angled out of the cupule (Fig. 1). Finally, the outer glume does not become as polished as a normal teosinte glume but has a duller surface, perhaps as a result of the disruption of normal cell differentiation on the glume surface (Fig. 4).

Analysis of *tga1* in the maize W22 genetic background revealed similar effects on ear development. In W22, *tga1* renders the glume more highly indurated, polished, more rounded, and pointed upward toward the apex of the ear (Fig. 5). Surrounding the kernel in this manner, the glume, as it develops and hardens, constricts the developing maize kernel, distorting its shape and often causing it to crack as it matures. As in the teosinte background, *tga1* in W22 causes greater elongation of the internodes (rachids) that compose the cob. This allele also renders the maize ear more susceptible to smut and mold and results in reduced seed set.

The effects of *tga1* in the maize background are rather severe and reduce the utility of maize as a grain crop. If teosinte is ancestral to maize, then *Tga1* must represent a major step in maize evolution because without it maize would be a far less useful crop. The effects of the maize allele in the teosinte background seem less severe. This genetic combination results in shorter ears that remain protected in the husks, and we observed no increased propensity for smut infections. The maize allele does expose the mature kernels, once removed from the husk, to pests. Although this exposure would affect fitness for a wild species, it should not be a problem for kernels harvested by humans and stored safely away from potential pests.

The discovery of *tga1* elucidates one of the probable steps in the transformation of teosinte into maize. This finding also provides evidence for the view that the maize ear was derived from the teosinte ear by a series of modifications, each principally controlled by one or two genes (*7*). An alternate proposal that the maize ear was derived by feminization of a central tassel spike and that soft glumes were an automatic result of feminization because tassel spikelets have soft glumes cannot be reconciled with our results (*9*). In fact, a condition of the latter view is that a locus such as

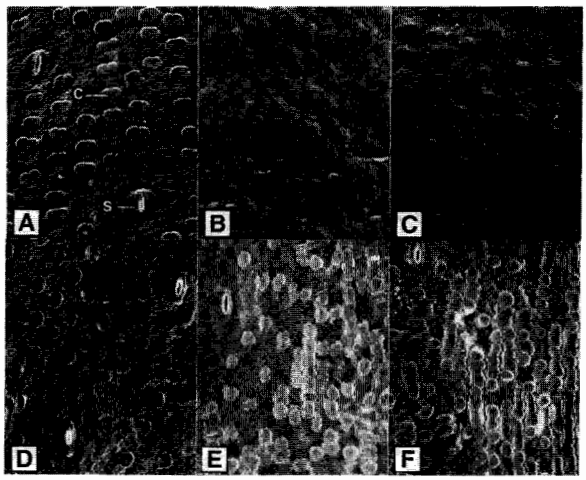

Fig. 4. Scanning electron micrographs of the surface of the outer glume of (**A** to **C**) the ear of teosinte and (**D** to **F**) of teosinte homozygous for the maize allele at *tga1*. Glume surfaces (A and D) just before pollination and approximately (B and E) two and (C and F) five weeks post-pollination are shown. In teosinte, the short cells (c) are arranged in distinct rows (A) and the glume epidermis forms a smooth regular surface as it matures (B and C). The maize allele at *tga1* appears to alter both the arrangement of short cells and the formation of a smooth regular surface at maturity (F). Stomata (s) are visible before pollination in teosinte but are obscured as the glume matures (B and C). With the maize allele at *tga1*, the stomata remain visible even in the mature glume (F). The scale bar represents 50 micrometers.

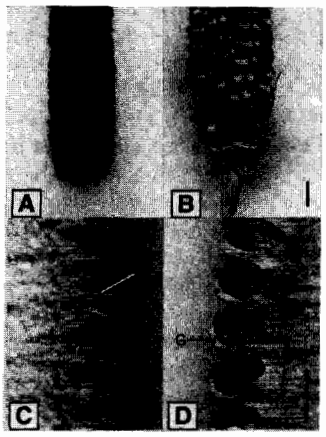

Fig. 5. Mature ears (without kernels) of maize line W22 homozygous for the (**A** and **C**) maize and (**B** and **D**) teosinte alleles at *tga1*. With the maize allele (A), the relatively small outer glumes are not visible, obscured by the pigmented bracts (paleas and lemmas). With the teosinte allele (B), the paleas and lemmas are obscured by the enlarged, unpigmented outer glumes. Longitudinal cross-sections show that W22 with the maize allele at *tga1* has outer glumes that are thin and perpendicular to the axis of the ear (C), whereas those of W22 with the teosinte allele at *tga1* are thicker and curved upward (D). The scale bar in (B) represents 1 cm and applies to both (A) and (B); the scale bar in (D) represents 5 mm and applies to both (C) and (D).

tga1 should not exist (9). The discovery of *tga1* also represents a case in which the evolution of a new adaptation was largely governed by a single locus, providing further evidence for the controversial view that evolution can proceed by a relatively few large steps (*13*). Because the development of Native American societies and the evolution of maize were intimately connected (*14*), the selection of *Tga1* by early maize agriculturists represents a critical event in the cultural history of the New World.

REFERENCES AND NOTES

1. G. W. Beadle, *Field Mus. Nat. Hist. Bull.* **43**, 2 (1972).
2. W. C. Galinat, *Annu. Rev. Genet.* **5**, 447 (1971).
3. J. F. Doebley, M. M. Goodman, C. W. Stuber, *Syst. Bot.* **9**, 203 (1984).
4. H. H. Iltis and J. F. Doebley, *Am. J. Bot.* **67**, 994 (1980).
5. T. A. Kato, *Res. Bull. Mass. Agric. Exp. St.* **635**, 1 (1976).
6. B. McClintock, T. A. Kato, A. Blumenschein, *Chromosome Constitution of Races of Maize* (Colegio de Postgraduados, Chapingo, Mexico, 1981).
7. G. W. Beadle, *J. Hered.* **30**, 245 (1939); *Sci. Am.* **242**, 112 (January 1980).
8. W. C. Galinat, *Maydica* **30**, 137 (1985).
9. H. H. Iltis, *Science* **222**, 886 (1983).
10. J. F. Doebley, A. Stec, J. F. Wendel, M. Edwards, *Proc. Natl. Acad. Sci. U.S.A.* **87**, 9888 (1990); J. F. Doebley and A. Stec, *Genetics* **129**, 285 (1991); ———, *ibid.* **134**, 559 (1993).
11. P. C. Mangelsdorf, *Adv. Genet.* 1, 161 (1947); J. S. Rogers, *Genetics* **35**, 541 (1950); W. C. Galinat, *Econ. Bot.* **17**, 51 (1963).
12. Of the 212 progeny, there were 142 nonindurate and 70 indurate types. These numbers deviate from the expected 3:1 segregation ratio for a locus with dominant gene action. The RFLP loci deviated in the same fashion; for example, *UMC191* had a 27:113:90 ratio of maize homozygotes:heterozygotes:teosinte homozygotes, which deviates from the expected 1:2:1 segregation ratio for a codominant locus. These deviations reflect the different allelic constitutions of W22 and W22-TGA for a gametophytic incompatibility locus (CP2) located near *tga1* [J. L. Kermicle and J. O. Allen, *Maydica* **35**, 399 (1990)]. Although *tga1* behaves like a qualitative locus in the uniform genetic background of W22, its phenotypic expression can be affected by unlinked loci, causing it to behave more like a QTL in a heterogeneous genetic background [J. F. Doebley, J. E. Dorweiler, J. L. Kermicle, *Maize Genet. Coop. Newsl.* **66**, 95 (1992)].
13. H. A. Orr and J. A. Coyne, *Am. Nat.* **140**, 725 (1992).
14. K. V. Flannery, *Annu. Rev. Anthropol.* **2**, 271 (1973); C. B. Heiser, *Seed to Civilization: The Story of Food* (Freeman, San Francisco, CA, 1981), pp. 100–101.

15. We thank B. Burr, K. Cone, J. Gardiner, D. Grant, C. Hannah, and J. Rosichan for providing RFLP probes. Supported by National Science Foundation grant BSR9107175 and by the Charles J. Brand Fellowship (J.D.).

8 April 1993; accepted 18 August 1993

Mammalian Locomotor-Respiratory Integration: Implications for Diaphragmatic and Pulmonary Design

Dennis M. Bramble* and Farish A. Jenkins Jr.

Diaphragmatic function and intrapulmonary respiratory flow in running mammals were found to differ substantially from the corresponding conditions known in resting mammals. In trotting dogs, orbital oscillations of the diaphragm were driven by inertial displacements of the viscera induced by locomotion. In turn, oscillations of the visceral mass drove pulmonary ventilation independent of diaphragmatic contractions, which primarily served to modulate visceral kinetics. Visceral displacements and loading of the anterior chest wall by the forelimbs are among the factors that contribute to an asynchronous ventilation of the lungs and interlobar gas recycling. Basic features of mammalian respiratory design, including the structure of the diaphragm and lobation of the lungs, appear to reflect the mechanical requirements of locomotor-respiratory integration.

Mammals, among the most active of vertebrates, have evolved respiratory and locomotor systems of complex and distinctive design. Despite substantial interest focused on the mechanical basis of mammalian respiration, numerous aspects of the respiratory system, including diaphragmatic structure, pulmonary lobation, and right-left asymmetry of the lungs, are as yet poorly understood. In reality the thoracic complex of mammals is inextricably linked to both respiration and locomotion, and the demands of both are intensified during exercise (*1*). Reptiles, in contrast, appear unable to achieve effective lung ventilation during rapid locomotion; a mechanical constraint on simultaneous running and breathing is probably primitive for tetrapods (*2*). The ability to integrate locomotor and respiratory mechanics appears to be an evolutionarily derived feature that has been critical to developing the elevated aerobic capacity and stamina that distinguishes mammals and birds (*2*, *3*).

In stationary mammals, contraction of the diaphragm provides a primary mechanical drive for inspiration. In running mammals, inertial oscillations of the abdominal viscera and the movements of the trunk have been hypothesized as influencing diaphragmatic mechanics in a manner that tends to synchronize respiration with locomotion (*4*). Observations of coupling ratios between breathing and gait cycles in various mammals have been cited in support of such a mechanical integration (*1*, *5*), but the significance of this phenomenon has remained controversial (*6*) in the absence of direct observations of diaphragmatic or visceral motion in active animals. We present a cineradiographic analysis of diaphragmatic, trunk, and chest wall movements in trotting dogs (*7*) and infer previously unknown patterns of gas flow within the lungs that result from locomotor-respiratory interactions.

In trotting, contralateral pairs of fore- and hindlimbs alternate in providing support and propulsion. Cyclical variations in vertical and horizontal accelerations of the body occur in conjunction with the contact phase of each limb pair. During the initial part of the contact phase (Fig. 1, phases A and B), the trunk sinks downward, decelerating horizontally and vertically (Fig. 1, G through I); during the second half of the contact phase, the body accelerates upward and forward (Fig. 1, G through I; phases B and C). Although the acceleration-deceleration profiles are consistent for all dogs, the vertical oscillations, which occur twice in each stride cycle, are not invariably symmetric; greater vertical excursion commonly occurs during the contact phase of a particular forelimb (usually the right) (Fig. 1G). The displacements of the diaphragm appear to result primarily from the inertial oscillations of the pendulous visceral mass within the abdomen and in particular the liver, which is attached centrally to the diaphragm. When the trunk decelerates during the initial part of a contact phase, the viscera displace the diaphragm craniad (Fig. 1J; phases A and B). Conversely, when the trunk subsequently accelerates forward and upward, the diaphragm follows the visceral mass caudad (Fig. 1J; phases B and C). As expected, the primary respiratory cycle of inspiration and expiration closely tracks the movements of the oscillating diaphragm (Fig. 1K) (*8*).

Excursions of the viscera during trotting are affected not only by the kinetic oscillations of the trunk but also by the physiological state of the diaphragm, which we infer from cineradiographic observations. Excursions of the inactive diaphragm are larger than those during contractions

D. M. Bramble, Department of Biology, University of Utah, Salt Lake City, UT 84112.
F. A. Jenkins Jr., Department of Organismic and Evolutionary Biology, and Museum of Comparative Zoology, Harvard University, Cambridge, MA 02138.

*To whom correspondence should be addressed.